PHYSICAL REVIEW B VOLUME 23, NUMBER 7 1 APRIL 1981

Solid solutions under irradiation. II. Radiation-induced precipitation in AlZn undersaturated solid solutions

R. Cauvin and G. Martin
Centre d'Etudes Nucléaires de Saclay, Section de Recherches de Métallurgie Physique, 91191 Gif-sur-Yvette Cèdex, France
(Received 5 May 1980)

A systematic study of radiation-induced Zn precipitation in undersaturated Al-Zn solid solutions is presented. Zn solubility in Al may be drastically decreased by high-flux 1-MeV electron irradiation (e.g., by a factor greater than 10 at 235 °C under 2.5×10^{20} $e\,cm^{-2}s^{-1}$). The shape and location of the Zn solvus in the AlZn phase diagram is flux dependent. The precipitate volume fraction does not obey the lever rule when applied to the solvus under irradiation. The above features are well accounted for by the model for radiation-induced solid-solution metastability presented in I. According to this model, the irreversible vacancy-interstitial mutual recombination is at the root of the destabilization of the solid solution by irradiation. We therefore suggest that radiation-induced precipitation in this system is an example of a nonequilibrium phase transition.

I. INTRODUCTION

Several studies are now available in which irradiation by energetic particles is shown to induce second-phase precipitation in solid solutions which are *undersaturated* outside irradiation. The main examples of such radiation-*induced* (as opposed to accelerated) precipitation are listed in paper I of the present work.[1]

In the AlZn system, radiation-induced precipitation (RIP) was reported to exhibit several interesting features which were not expected on the basis of the existing theories.[2] In Al-1.9 at.% Zn, under high-flux 1-MeV electron irradiation, Zn precipitation was observed: (i) to be *homogeneous*, i.e., not associated with point-defect sinks, contrary to what is observed in NiBe,[3] NiSi,[4–6] and NiGe[7]; (ii) to be *coherent* [in the form of Guinier-Preston (GP) zones] as well as *incoherent* (hcp Zn precipitates) contrary to what was predicted by the available model of homogeneous precipitation which predicts RIP for incoherent precipitates only[8]; (iii) with a *precipitate atomic volume* smaller than that of the matrix, contrary to what was expected from the latter model[8]; and (iv) to occur at temperatures below a flux-dependent temperature threshold.

Together with the above experimental evidence, we had shown on a simple model that the irreversible vacancy-interstitial mutual recombination reaction may be at the origin of the amplification of solute concentration fluctuations in solid solutions under irradiation. AlZn was a good candidate for such a phenomenon since Zn is known to attract vacancies as well as interstitials and the coupling coefficients between Zn flux and vacancy (respectively, interstitial) flux are known (respectively, predicted) to be positive which is one of the cases where radiation-induced amplification of solute concentration fluctuations is expected to occur according to the proposed model.[2] Due to the extreme simplicity of the latter model, no quantitative check could be made.

The purpose of this paper is twofold: We first present a systematic study of the irradiation conditions which induce precipitation in undersaturated AlZn solid solutions, over a wide range of solute concentrations. As a result of this study, the solvus of Zn in Al is determined as a function of the irradiation flux. Moreover an estimate of the precipitate volume fraction yields the interesting result that precipitation saturates despite the fact that the solute content of the matrix between the precipitates is greater than the solubility limit under irradiation. The experimental results are presented in Sec. II.

In Sec. III, we briefly report attempts to interpret the results of Sec. II by existing models. We first show that the results cannot be interpreted on a strictly thermodynamical basis. Then we show that the extension which we had suggested[2] for the incoherent RIP model of Maydet and Russell[8] to apply to undersized precipitates does not account for our results. On the other hand, we show that the experimental results are well interpreted by the model of radiation-induced metastability presented in Paper I.[1] The quantitative assessment of the model requires first an estimate of the point-defect supersaturation in the alloy under irradiation. We then proceed with the computation of the solvus under irradiation and of the departure from the lever rule for the precipitate volume fraction. The sensitivity of the results to the values of the experimental parameters is checked.

Finally we discuss the refinements to be brought to our model of metastability (Paper I) in order to improve the quantitative agreement with our results.

II. EXPERIMENTAL STUDY OF RIP IN AlZn

A. Experimental procedure

Al-Zn solid solutions with nominal composition of 0.2, 0.6, 0.8, 1.9, and 4.4 at.% Zn were studied. The three more dilute solutions were produced from high-purity Al and Zn using a levitation technique under argon atmosphere. The two more concentrated alloys were kindly provided by PUK company and contained less than 300 wt. ppm overall impurity according to the manufacturer's analysis. The alloys are cold rolled to 150-μm-thick sheets. Further treatments are described elsewhere.[2]

Irradiations were performed with 1-MeV electrons in a high-voltage electron microscope (HVEM), either at CNRS-ONERA, Paris, or at MPI-Stuttgart where the better resolution of the AEI microscope allows for an *in situ* observation of the precipitation process. (We are indebted to Dr. K. Urban for giving access to the microscope of MPI Stuttgart.)

Prior to irradiation, the specimens were given an *in situ* annealing treatment, in the hot stage of the microscope at temperatures well above the solvus temperature. According to Hansen,[9] the solvus temperature is, respectively, 45°, 110°, and 175 °C for alloy composition of 0.8, 1.9, and 4.4 at.% Zn. These latter alloys were preannealed for half an hour at 235 or 250 °C. For the more dilute alloys (0.2 and 0.6 at.% Zn) the solvus temperature is below room temperature; moreover, these alloys degrade rapidly at high temperature in the microscope. Therefore the preannealing treatment was performed at the irradiation temperature only. Control experiments performed on 0.8 at.% Zn alloys convinced us that the effects of irradiation which we are interested in, were not affected by the type of preannealing treatment used. Nevertheless, performing observations on 0.2 and 0.6 at.% Zn alloys was always more difficult than on more concentrated alloys.

B. Irradiation conditions leading to Zn precipitation

The type of radiation damage observed was described previously.[2] For appropriate temperatures and irradiation fluxes, Zn precipitates appeared. These were either coherent spherical GP zones or incoherent hcp Zn platelets.

As previously, we checked, whenever it was possible, that the precipitates were well inside the foil and not a surface effect, and would redissolve during a post irradiation anneal at the irradiation temperature. This latter check could be performed down to 135 °C.

As far as Zn precipitation is concerned, Table I summarizes the experimental data for the alloys with 0.2, 0.6, 0.8, 4.4 at.% Zn. The results concerning the 1.9 at.% Zn composition were reported previously.[2] As can be seen, the irradiation temperatures range from 100 to 250 °C and the irradiation fluxes from 1.01 to 25.2×10^{19} $e\,cm^{-2}s^{-1}$ which corresponds to defect production rates ranging from 6.3×10^{-4} to 1.5×10^{-2} dpa s^{-1} using the same conversion factors as previously (dpa is the displacement per atom). The above results permitted the construction of the Al rich side of the AlZn phase diagram under e irradiation (Fig. 1). The points on Fig. 1 either correspond to actual observations or to conclusions reached by interpolation of existing data. The solvus under irradiation is rather precisely defined by the data points for high-flux irradiation. For lower flux irradiations, the data are less abundant; when necessary, we made the assumption that no precipitates would form at low flux if none did form at high flux.

As shown by Fig. 1, large decrease of the Zn solubility is observed between 150 and 235 °C. For the higher temperatures, the location of the Zn solvus is

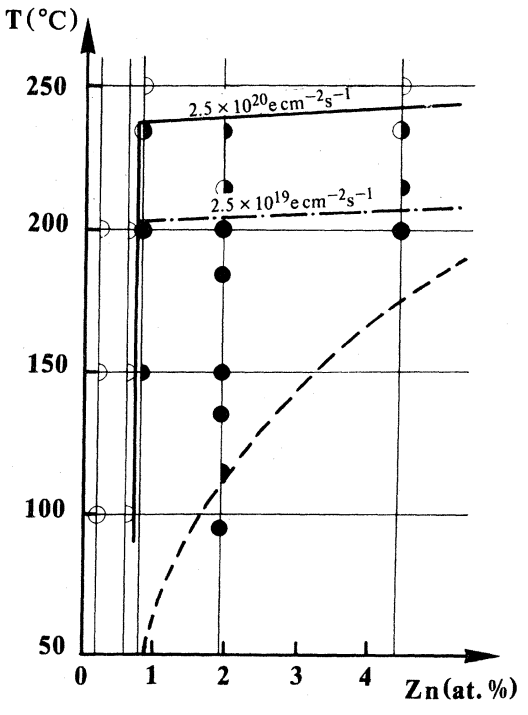

FIG. 1. Experimental Zn solvus in Al under 1-MeV electron irradiation. —— High-flux (2.5×10^{20} $e\,cm^{-2}s^{-1}$); —·— Low-flux irradiation (2.5×10^{19} $e\,cm^{-2}s^{-1}$). Precipitation: ◗ observed, ◗ not observed under ◖ low-flux, ◖ high-flux irradiation.

TABLE I. Experimental observations: $\vec{k}_0$ is the direction of the electron beam during irradiation.

[Zn] (at.%)	T (°C)	$10^{19}\phi$ (e cm^{-2}s^{-1})	$10^4 G$ (dpa s^{-1})	Gt (dpa)	$\vec{k}_0$	Precipitation observed
0.2	100	10.5	64.1	34.6	[110]	No
· · ·	100	3.5	21.3	7.69	· · ·	No
· · ·	150	7.6	46.4	16.7	· · ·	No
· · ·	200	5.0	30.5	11.0	· · ·	No
0.6	100	19.5	119	42.8	· · ·	No
· · ·	150	19.0	116	41.7	[100]	No
· · ·	200	18.5	113	30.5	[110]	No
0.8	150	21.3	130	70.2	· · ·	Yes
· · ·	200	24.1	147	8.82	· · ·	Yes
· · ·	200	8.06	49.2	4.43	· · ·	Yes
· · ·	200	2.56	15.6	2.81	· · ·	Yes
· · ·	235	24.4	149	8.93	· · ·	Yes
· · ·	235	8.43	51.4	9.26	· · ·	No
· · ·	250	24.7	151	27.1	· · ·	No
4.4	200	21.9	134	60.1	· · ·	Yes
· · ·	200	4.26	26.0	9.36	· · ·	Yes
· · ·	200	1.01	6.26	0.55	· · ·	Yes
· · ·	215	21.3	130	23.4	· · ·	Yes
· · ·	235	25.2	154	46.1	· · ·	Yes
· · ·	235	8.43	51.4	18.5	[100]	No
· · ·	250	24.8	151	54.5	· · ·	No

strongly flux dependent: the solvus temperature is increased by roughly 35 °C for one order of magnitude increase of the irradiation flux.

C. Precipitate volume fraction

In the course of *in situ* observations of the precipitation process, and for large total dose experiments, we were struck by the fact that the precipitate volume fraction appeared to saturate in the range of 10^{-3}, whatever the sample composition and despite the fact that the irradiation was continued approximately twice as long as was necessary to reach the apparent saturation. To make this observation more precise, we performed a quantitative determination of the β-Zn precipitate volume fraction in samples with 0.8 at.% Zn irradiated at 200 and 235 °C under high-flux conditions (2.4×10^{20} e cm^{-2}s^{-1}) and in samples with 4.4 at.% Zn irradiated at 200, 215, and 235 °C under, respectively, 2.19, 2.13, and 2.5×10^{20} e cm^{-2}s^{-1}. The foil thickness was determined by stereomicroscopy; the precipitate sizes were measured on front views and edge on pictures. The precision of the measurement of the precipitate volume fraction is low (±25%) but sufficient to confirm our first impression as shown in Fig. 2: in the Al-0.8 at.% Zn, the precipitation proceeds until the solute content of the matrix between the precipitates reaches the solubility limit (0.7 at.%). This is not the case on the 4.4 at.% Zn solid solution: the precipitation saturates while the matrix composition is still larger than the Zn solubility limit under irradiation.

Therefore the solvus under irradiation which is depicted on Fig. 1 is simply the boundary between the single-phase and the two-phase field in the temperature versus composition diagram. It does not indicate what the concentration of the matrix is in the presence of precipitates.

This observation, which seems at first surprising, is well accounted for by the model proposed in the first part of this work.[1] In a general way, one should keep in mind that a system under irradiation is an open system for point defects, sustained in a dynamical state by the irradiation flux. It is a rather general feature of such systems that the state which they reach depends on the boundary conditions which prevail: the system must be treated as a whole and cannot be divided into subsystems without care.

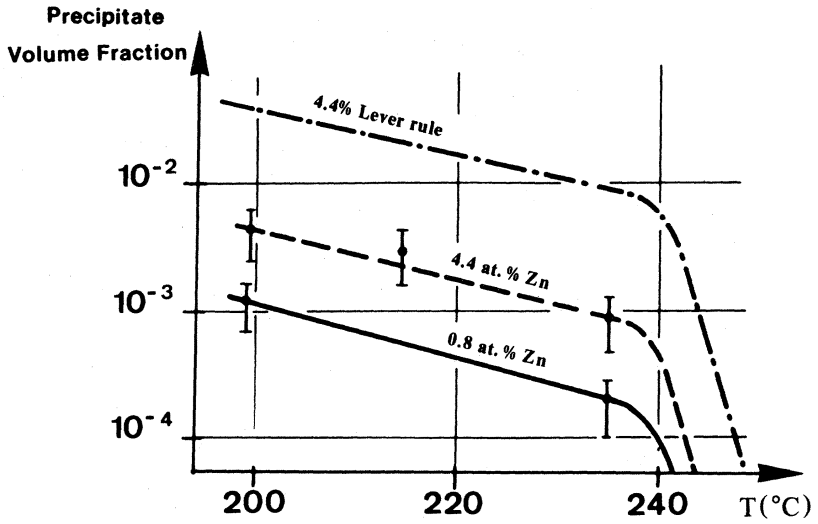

FIG. 2. Precipitate volume fraction after high dose irradiation. The irradiation conditions are specified in Table I (larger dose irradiations).

III. INTERPRETATION OF THE DATA

As discussed previously,[10] radiation-induced precipitation may be given either a static or a kinetic interpretation. In the static interpretation one simply claims that the radiation-induced point-defect supersaturation contributes sufficiently to the free energy of the solid solution to render it unstable as compared to the two-phase alloy. In the kinetic interpretations, the nonconservative nature of point defects is taken fully into account. In this section we show that unlike other interpretations, the kinetic model presented in Paper I[1] accounts well for the above results.

A. Failure of a static interpretation

The various attempts to account for radiation-induced precipitation by a strictly thermodynamical argument have been listed in the first part of this work. Here we restrict ourselves to the semiempirical approach of Gittus and Miodownik, which allows for a quantitative check of the approach.[11] According to these authors, a lower bound of the free-energy increase (ΔG) of the solid solution which is necessary to account for the occurrence of second-phase precipitation may be obtained by the construction depicted in Fig. 3. When applied to available AlZn thermodynamical data[12,13] the latter construction yields a

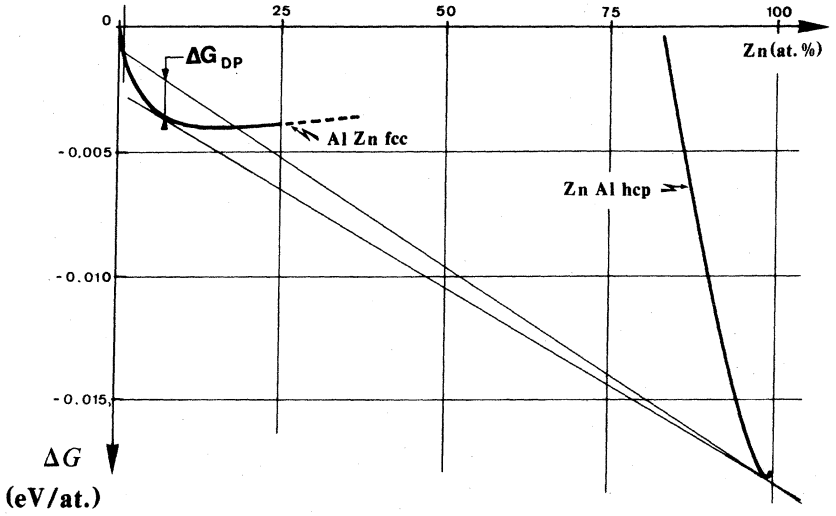

FIG. 3. Graphical estimation on the free energy alteration of the AlZn solid solution necessary to trigger Zn precipitation out of Al-0.7 at.% Zn at 235 °C.

value of $\Delta G > 1.1 \times 10^{-3}$ eV per atom at 235 °C, to account for a solubility limit of 0.7 at.% Zn under high-flux irradiation. Under such irradiation conditions, the point-defect concentrations are estimated (cf. Sec. III B) to be 10^{-5} vacancy and 10^{-8} interstitial per atom for a displacement rate of 2×10^{-2} dpa s^{-1}. The above concentrations include free and trapped defects. Since the vacancy (respectively, interstitial) formation energy is known (respectively, estimated) to be 0.66 eV (Ref. 14) [respectively 3.2 eV (Ref. 15)], it is obvious that the strictly static approach just described fails by two orders of magnitude to account for the data.

B. Failure of available kinetic models

As was suggested by Maydet and Russell[8] and Saiedfar and Russell,[16] the elimination of point defects at a precipitate-matrix interface may promote precipitation by relaxing the misfit energy which develops whenever matrix atoms are replaced by precipitate atoms with different atomic volume. The effect of the point-defect supersaturation may be split into two terms: a first-order one which shows that oversized precipitates may form in undersaturated solid solutions under irradiation while undersized precipitates would dissolve in supersaturated solid solutions under irradiation, and a second-order term which might account for radiation-induced precipitation of undersized precipitates.[2,17]

We performed a quantitative assessment of the latter effect using the same parameters as in Sec. III C for the evaluation of the point-defects supersaturation and mobilities. The results are given in Fig. 4. As can be seen, in the region of interest, the first-order effect of the vacancy supersaturation dominates, therefore *increasing* the solubility of Zn in Al. The second-order effect only shows up at low temperature for very high defect concentrations. As is clear from Fig. 4 the model just discussed does not account for the results presented in Sec. II.

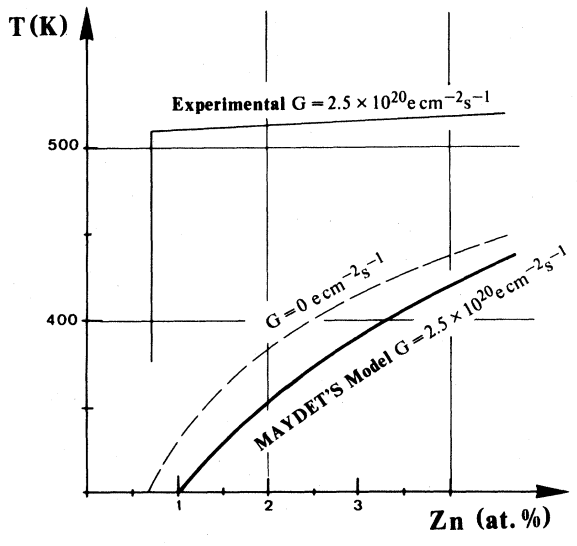

FIG. 4. Zn solvus under irradiation as estimated from the available incoherent precipitation model (Ref. 8): the bias for point-defect capture at dislocations is taken equal to 0.1.

C. Quantitative assessment of the model of recombination-induced solid-solution metastability

As discussed in the first part of this work,[1] under appropriate conditions, the solubility limit under irradiation $\tilde{C}$ may be deduced from the thermodynamical solubility limit $\bar{C}$ by

$$\tilde{C} = \bar{C}B \quad . \tag{1}$$

B is the parameter defined a:

$$B = \left[1 + \left[\frac{D_s^i}{D_s^v}\right]^X\right]^{-1} \quad , \tag{2}$$

where D_s^v and D_s^i are the solute diffusion coefficients, respectively, by vacancy and interstitial mechanisms, and $X = -1$ if the occupation probability of an interface site by a point defect is larger for an interstitial than for a vacancy and $+1$ when the reverse is true. $X = +1$ in the present experiment as will be seen in Sec. III C 3. In the limit of weak trapping energies, the latter probabilities are given by

$$p_i = c_i \exp(-g_i^B/kT) \quad , \tag{3a}$$

$$p_v = c_v \exp(-g_v^B/kT) \quad , \tag{3b}$$

where c_i and c_v are the free interstitial and free vacancy concentrations and g_i^B and g_v^B the binding free energies of interstitials and vacancies at the precipitate matrix interface ($g^B < 0$ for an attraction).

In order to evaluate the solubility limit under irradiation [$\tilde{C}$ in Eq. (1)], we need an evaluation of the point-defect concentrations and of the solute diffusion coefficients for various irradiation conditions and solute content of the solid solution. In the following we briefly describe the method used, and the quantitative results. The details are given in the Appendixes.

1. *Solute diffusion coefficients under irradiation*

Following Howard and Lidiard[18] it is simple to show that the solute diffusion coefficient by vacancy mechanism in a dilute alloy is directly proportional to the free vacancy concentration [cf. Appendix A Eqs.

(A8) to (A20)].

Assuming that the five vacancy jump frequencies which enter Howard and Lidiard's model are not affected by irradiation yields the simple result that the solute diffusion coefficients by vacancy mechanism under irradiation $D_s^v(\phi,T)$ and without irradiation $D_s^v(0,T)$ are scaled by the free vacancy supersaturation

$$D_s^v(\phi,T)=D_s^v(0,T)S_v(\phi,T) \quad , \tag{4}$$

where

$$S_v(\phi,T)=C_v(\phi,T)/C_v(0,T) \quad . \tag{5}$$

$D_s^v(0,T)$ has been determined experimentally.[19,20] According to Eq. (5) we simply need the vacancy supersaturation in order to estimate $D_s^v(\phi,T)$, from the experimental value of $D_s^v(0,T)$.

An expression similar to Eq. (4) has been proposed recently[21] for the impurity diffusion coefficient by interstitial mechanism, D_s^I, where the interstitial is assumed to be of the $\langle 100\rangle$ dumbbell type. The main difference between the expression of D_s^I and D_s^v is that more numerous jump frequencies are necessary for describing the migration of a solute atom by an interstitial mechanism. Moreover, no experimental data is available for D_s^I without irradiation. We must therefore rely, on numerical evaluations not only for p_i (as in the vacancy case for p_v) but also for the various jump frequencies involved in D_s^I. The latter jump frequencies are evaluated following the model of Dederichs and co-workers.[22] The advantage of this model is to scale all relevant jump frequencies with the aid of the solute misfit parameter. We are aware that it may be a very crude approximation.[23,24] It is nevertheless the only available guide in the absence of experimental data. Here again, we are left with the problem of evaluating p_i, i.e., the interstitial concentration.

We now turn to the evaluation of the vacancy and interstitial concentrations as a function of the irradiation flux and temperature, of the solute content and of the density of traps in the solid solution.

2. *Evaluating the point-defect concentration in the solid solution under irradiation: method*

In order to account for the various aspects of radiation-induced precipitation reported in Sec. II we need a careful description of point-defect production and elimination in the solid solution under irradiation. Once created, the point defects migrate as free defects, or as solute-defect complexes; they may annihilate by mutual recombination or at point-defect sinks (free surfaces, dislocation lines, etc.); they may also get trapped at immobile trapping centers, at the periphery of the solute clusters. All the above events must be included in the balance equations for point defects, since they enter the model of radiation-induced metastability. The balance equations must be treated with the same level of detail as the model they enter.

To our knowledge the problem so defined has not yet been treated. Two partial problems have been, however, treated in detail separately: the point-defect population in the presence of mobile solutes but in the absence of saturable traps,[25] and the complementary problem, saturable traps but no mobile solute.[26] In order to couple the two problems we propose the following scheme.

We divide the problem into two parts and consider (a) the solvent together with the single solute atoms (which form with point-defects mobile complexes) and (b) the solute clusters (which act as traps for the mobile species). Solvent plus single solute atoms are treated as an average medium according to a homogenization procedure described in Appendix A. In the frame of this mean-field approximation, we define average diffusion coefficients for the point defects ($\mathfrak{D}_v$ and $\mathfrak{D}_i$, respectively, for vacancies and interstitials). The coefficients are of course functions of the temperature and of the single solute concentration [Eqs. (A15) and (A21)]. In the average medium so defined, rate constants for defect mutual recombination, elimination at sinks, and trapping at trapping centers may be defined as functions of $\mathfrak{D}_v$ and $\mathfrak{D}_i$. We are left with the problem of evaluating point-defect populations in the presence of immobile trapping centers. As already discussed[25] this problem involves four balance equations, for trapped and untrapped vacancies and interstitials. More precisely, if $\mathcal{C}_v$, $\mathcal{C}_{vt}$, $\mathcal{C}_i$, $\mathcal{C}_{it}$, $\mathcal{C}_t$ are, respectively, the concentrations of untrapped and trapped vacancies and interstitials and of trapping centers, the following relationships hold at steady state:

$$\frac{\partial \mathcal{C}_v}{\partial t}=G+K_v'\mathcal{C}_{vt}-R_{iv}\mathcal{C}_i\mathcal{C}_v-R_{it}\mathcal{C}_v\mathcal{C}_{it} - K_v''\mathcal{C}_v(\mathcal{C}_t-\mathcal{C}_{vt}-\mathcal{C}_{it})-K_v(\mathcal{C}_v-\mathcal{C}_v^0)=0 \quad , \tag{6a}$$

$$\frac{\partial \mathcal{C}_i}{\partial t}=G+K_i'\mathcal{C}_{it}-R_{iv}\mathcal{C}_i\mathcal{C}_v-R_{vt}\mathcal{C}_i\mathcal{C}_{vt} - K_i''\mathcal{C}_i(\mathcal{C}_t-\mathcal{C}_{vt}-\mathcal{C}_{it})-K_i\mathcal{C}_i=0 \quad , \tag{6b}$$

$$\frac{\partial \mathcal{C}_{vt}}{\partial t}=K_v''\mathcal{C}_v(\mathcal{C}_t-\mathcal{C}_{vt}-\mathcal{C}_{it})-K_v'\mathcal{C}_{vt}-R_{vt}\mathcal{C}_i\mathcal{C}_{vt}=0 \quad , \tag{6c}$$

$$\frac{\partial \mathcal{C}_{it}}{\partial t}=K_i''\mathcal{C}_i(\mathcal{C}_t-\mathcal{C}_{vt}-\mathcal{C}_{it})-K_i'\mathcal{C}_{it}-R_{it}\mathcal{C}_v\mathcal{C}_{it}=0 \quad . \tag{6d}$$

G is the point-defect production rate, K_v' and K_v'' the

detrapping and trapping coefficients of vacancies (equivalently K_i' and K_i'' for interstitials), R_{iv} the mutual recombination coefficient for untrapped vacancies and interstitials, R_{it} the coefficient of the recombination reaction of a trapped interstitial with a vacancy, R_{vt} that for a trapped vacancy with an interstitial, K_v and K_i the elimination constant of vacancies and interstitials at point-defect sinks, and C_v^0 is the thermal equilibrium vacancy concentration. As can be seen from Eq. (6), the trapping centers are assumed to be saturated once a single defect is trapped. With the not too restrictive assumption that the capture radii for a vacancy or interstitial of a free or saturated trap are equal, it is simple to show (cf. Appendix B) that

$$K_i \mathcal{C}_i = K_v(\mathcal{C}_v - \mathcal{C}_v^0) \tag{7}$$

and that $\mathcal{C}_v$ is the solution of

$$\mathcal{C}_v^4 + a_1\mathcal{C}_v^3 + a_2\mathcal{C}_v^2 + a_3\mathcal{C}_v + a_4 = 0 \ . \tag{8}$$

The expressions of a_1 to a_4 are given in the Appendix B.

Equations (8) and (7) yield the steady-state overall concentrations of untrapped defects in the average medium (solvent plus single solute atoms).

As discussed in Sec. III C, what we are looking for in order to make the connection with paper I of this work, is the concentration of free interstitial c_i, and free vacancies c_v in the solid solution, i.e., the concentration of those defects which are trapped neither on fixed trapping centers, nor on mobile single solute atoms. These latter concentrations are readily obtained from $\mathcal{C}_i$ and $\mathcal{C}_v$ since

$$c_v = \mathcal{C}_v/(1 + k_v c_B) \ , \tag{9a}$$

$$c_i = \mathcal{C}_i/(1 + k_i c_B) \ , \tag{9b}$$

where c_B is the concentration of single solute atoms and k_i and k_v are defined in Appendix A [Eqs. (A4) and (A32)]. In Eqs. (9a) and (9b), c_B is assumed to be much larger than the number density of solute-defect complexes.

The computation proceeds in two steps. We first deal with the precipitate free solid solution, for which we assume that the solute is mainly in the form of single solute atoms. We set therefore c_B equal to the nominal solute content of the solid solution and $\mathcal{C}_t = 0$ in Eqs. (6a) to (6d). From c_v and c_i deduced by solving Eqs. (8), (7), (9a), and (9b), we obtain p_i and p_v [Eqs. (3a) and (3b)], D_s^v, and therefore the solubility limit $\tilde{C}$ according to Eqs. (2) and (1). We must use an iterative procedure in order to evaluate D_s^i and D_s^v precisely for that solute content $\tilde{C}$ which yields a solubility limit equal to $\tilde{C}$.

In the next step we assume that some precipitation occurred. Therefore c_B is slightly less than the overall solute content of the system, but most important, $\mathcal{C}_t$ is now finite. The existence of fixed traps ($\mathcal{C}_t$) reduces the free-defect concentration: a modification of D_s^i and D_s^v results. As a consequence the solubility limit $\tilde{C}'$ in the matrix in presence of precipitates is found to be larger than that without the precipitates. We therefore get an explanation for the violation of the lever rule for the precipitate volume fraction, which was reported in Sec. II C. As shown next, the above computation scheme yields a good quantitative interpretation of the data reported in Secs. II B and II C.

TABLE II. Input parameters of the model. For vacancy diffusion data analysis, see Appendix A Sec. 2.

Vacancy	Formation energy	0.66 eV	Ref. 14
	entropy	$3.12k_B$	
	Migration energy	0.65 eV	
	Attempt frequency	5.6×10^{13} s^{-1}	From Debye frequency ν_D
	Solute binding energy	0.02 eV	Ref. 27
	entropy	$-4.0k_B$	
Interstitial migration energy		0.115	Ref. 28
	Attempt frequency	7×10^{12} s^{-1}	$\frac{1}{8}\nu_D$ according to Ref. 22
	Solute binding energy	See text	From Ref. 22
Linear misfit of Zn in Al		-0.02	Ref. 29
Dislocation density		10^{11} cm^{-2}	Equivalent to 1000-Å foil thickness
Zinc diffusion data by vacancy mechanism			
in pure Al			Ref. 19
Idem in Al-Zn alloys			Ref. 20
Interstitial-vacancy mutual recombination radius		$r_0 = \frac{5a}{2\sqrt{2}}$	Ref. 32
Young's modulus of Al		$E = 7.06 \times 10^{10}$ J m^{-3}	Refs. 30,31

3. *Numerical results*

The input parameters of the computation are the control parameters of the system (temperature, point-defect production rate, solute content), and materials characteristics: formation and migration energies of interstitials and vacancies, solute-defect binding energies, various defect jump frequencies. The values used and their sources are given in Table II. For the sink and trap densities the experimentally observed values are taken although they should be determined by a complete theory of the microstructural evolution of the solid solution under irradiation.

For the sake of simplicity we used the free solute-defect binding energy as a binding energy of defects to immobile traps. As a result, under the irradiation conditions used, we find, that the trapping centers are more probably occupied by vacancies than by interstitials [$x = +1$ in Eq. (2)]. This occurs because of the low free interstitial concentration in spite of the larger binding energy of interstitials than that of vacancies to traps.

The main results of the numerical study are depicted in Figs. 5(a)–5(e).

(i) In Fig. 5(a), the computed solvus is compared to the experimental one. As can be seen, the effect of irradiation as calculated is larger than the experimentally observed effect. But the model yields the right shape for the solvus, and the right order of magnitude. The agreement with experimental data can be improved significantly, simply by reducing the solute misfit η by a factor 2, when computing the various interstitial jump frequencies according to the Dederichs *et al.* model[22] as was suggested in Ref. 33. To be fair one must recognize that the solute-interstitial binding energy which results is rather low compared to the 0.45 eV usually accepted[34] and recently found using pseudopotential calculations[24] whereas the right order of magnitude is obtained with $\eta = -2 \times 10^{-2}$.

(ii) As shown by Fig. 5(a), one order of magnitude

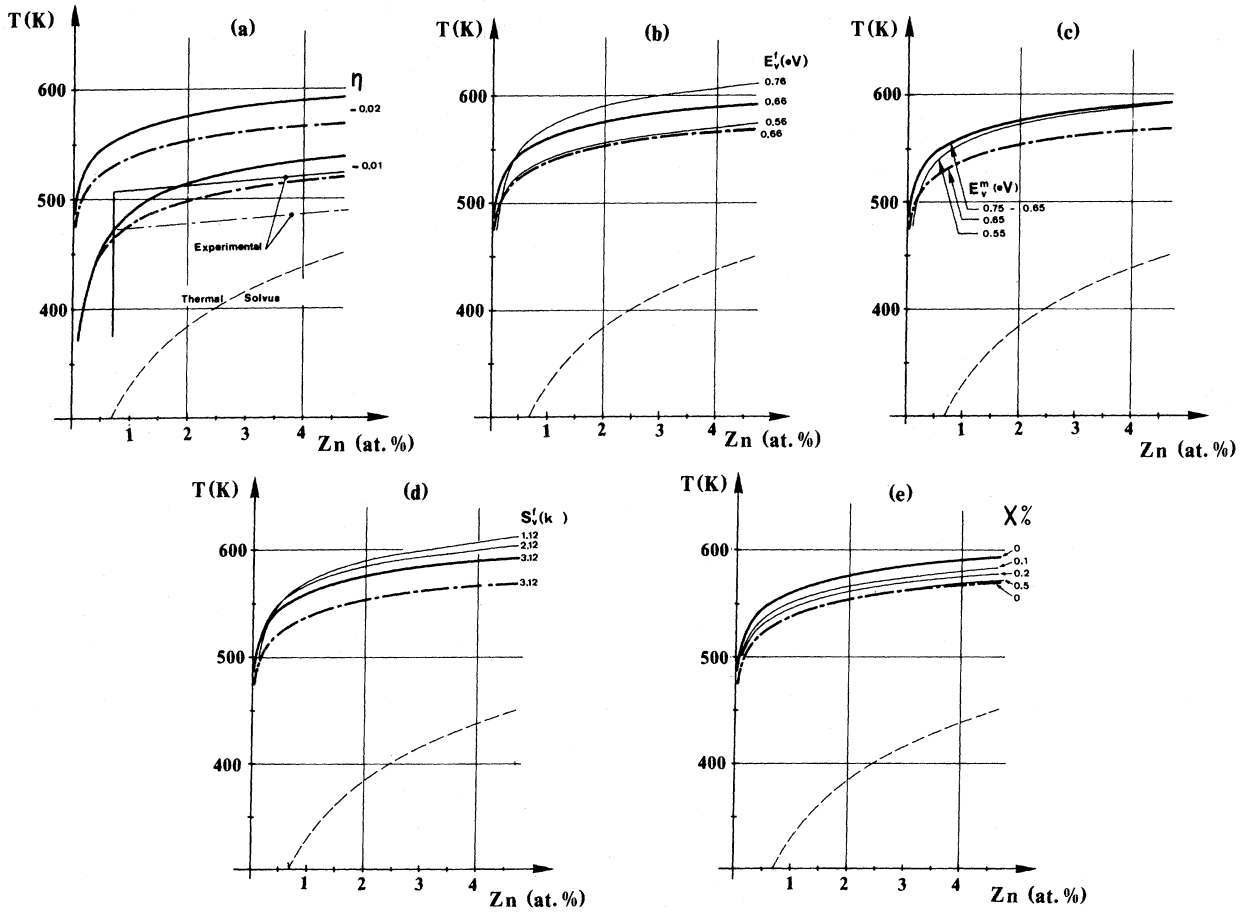

FIG. 5. Quantitative assessment of the model. For all figures: —— 2×10^{-2} dpa s^{-1}, —·— 2×10^{-3} dpa s^{-1}, —— —— —— no irradiation. (a) Computed solvus for two values of the solute linear misfit, compared to experimental solvus, (b) sensitivity of the solvus to the vacancy formation energy E_v^f, (c) sensitivity of the solvus to the vacancy migration energy E_v^m, (d) sensitivity of the solvus to the vacancy formation entropy S_v^f (k is the Boltzmann constant), (e) effect of the precipitate volume fraction (X) on the Zn solvus in the matrix between the precipitates.

drop of the irradiation flux depresses the upper solvus temperature by 25 °C, in fair agreement with the experiment (35 °C).

(iii) In the low concentration range (< 1 at.% Zn), the computed solubility limit is too low as compared to experimental data.

(iv) The sensitivity of the results to the values of the parameters is depicted in Figs. 5(b)–5(d). As can be seen, the most sensitive parameter is the vacancy formation energy, aside from the solute interstitial binding energy, the effect of which already appears in Fig. 5(a) (compare $\eta = -2 \times 10^{-2}$ and -1×10^{-2}). Vacancy migration energy and formation entropy are not very sensitive parameters [Figs. 5(c) and 5(d)]. In any case, the largest range of vacancy formation energies one can reasonably accept produces a change of the high-temperature threshold for radiation-induced precipitation equivalent to an uncertainty on the defect production rate by a factor 20 [Fig. 5(b)]. No sensitivity to the dislocation density was detected. The reason for this is the low vacancy formation energy in Al; the interstitial elimination is mainly by recombination with thermal vacancies in the temperature range where radiation-induced precipitation ceases.

(v) Finally Fig. 5(e) depicts the effect of the precipitate volume fraction on the residual solute content of the matrix. More precisely, assuming a precipitate volume fraction of 2×10^{-3} and a precipitate size such that the number of trapping centers at the periphery of the precipitate equals the number of solute atoms in the precipitate, the solvus depicted in Fig. 5(e) is obtained by the same procedure as before. As can be seen, a solid solution with 4.4 at.% Zn may be supersaturated in the absence of precipitates, and undersaturated with a 2×10^{-3} precipitate volume fraction, despite the fact that the residual solute content of the matrix is larger than the solubility limit in the absence of precipitation. As shown by Fig. 5(e), a precipitate volume fraction of 2×10^{-3} shifts the solubility limit by roughly the same amount as decreasing the irradiation flux by a factor of 8, in fair agreement with the data reported in Figs. 1 and 2: indeed, precipitation stops in a 4.4 at.% Zn solid solution, at 200 °C, under high-flux irradiation, when the precipitate volume fraction is a few times 10^{-3} (Fig. 2). As shown by Fig. 1, a decrease of the irradiation flux by a factor of 8 has the same effect, on a precipitate free 4.4 at.% Zn solid solution, as just computed.

IV. DISCUSSION

As just shown, the model of recombination-induced metastability proposed in Paper I, together with the computation scheme for the steady-state point-defect concentrations under irradiation accounts qualitatively and with the right order of magnitude for the two main observations reported in Sec. II, namely (i) the solid solubility of Zn in Al is decreased under high-flux 1-MeV e irradiation: the shape and location of the Zn solvus in the phase diagram is flux dependent; (ii) the "lever rule" for precipitate volume fraction is not obeyed under irradiation. Previously proposed models fail to account for these results. Nevertheless, our model overestimates the effect of irradiation as shown in Fig. 5(a). In this section we discuss the implication of this success and the origin of the remaining departure of the computed effect from experimental data.

A. Why does the model overestimate the effect of irradiation

As discussed in Paper I, the basic simplifying assumption of the model is that, when introduced in the solid solution, the point defects are trapped at preexisting solute clusters, without changing their equilibrium distribution, in the absence of interstitial-vacancy recombination. Moreover we assumed that defect clustering may be ignored. Finally the vacancy-interstitial recombination at the cluster is assumed to occur instantaneously.

The three above hypotheses certainly enhance the effect of irradiation. Indeed, if, e.g., interstitial-solute interaction is very large it may be *energetically* favorable for the solid solution to dissociate some large solute clusters in favor of solute-interstitial complexes: dissociating large solute clusters means improving the solid solution stability. Similarily, if defect clustering occurs, less defects (and therefore defect-solute complexes) reach the solute clusters: the driving force for solute clustering is decreased. Finally, if vacancy-interstitial recombination at solute clusters is not instantaneous, new reactions occur which were ignored in Paper I. For instance a finite probability exists that a solute cluster having one trapped interstitial reemits a solute after the impingement of a solute vacancy pair. This is not the case after vacancy-interstitial recombination. Here again the effect of the irreversibility of the vacancy-interstitial recombination is weakened.

It is therefore encouraging that the model as it was used, overestimates the effect of irradiation. Some difficulties indeed occur at lower irradiation temperature ($T < 100$ °C) where defect clustering is much more abundant as shown by some observations, the discussion of which is left for a future work. Work is in progress to include defect clustering in the model of Paper I.

B. What does the success of the model imply

The first point we can make is that the AlZn system in the temperature range depicted here does ful-

fill the simplifying assumptions of the model. Moreover, due to the failure of other theoretical approaches to account for the result, we may claim that the irreversibility of the vacancy-interstitial recombination is at the root of the destabilization of the AlZn solid solution. Radiation-induced precipitation in this system therefore offers one new example of so-called nonequilibrium phase transition in solid systems (cf. Ref. 22 in paper I).

From a more metallurgical view point, it might look surprising that the model proposed which dealt, strictly speaking, with coherent solute clusters does account for noncoherent precipitate stability under irradiation. First of all, in many cases where the precipitation process was slow enough, coherent GP zones form prior to Zn precipitates as already reported.[2] Nevertheless we think that the success of the model suggests the following remarks.

As discussed by several authors,[35,36] whenever the precipitate- and matrix-atomic volumes are different, the number of matrix lattice sites in the volume occupied by the precipitate must differ from the number of solute atoms in the precipitate, in order to cancel the strain in the system. Notice that the condition of zero strain energy is strictly fulfilled for some very precise cluster compositions defined according to the notation of paper I by

$$d^0 = -s\delta \ , \tag{10}$$

where s is the number of solute atoms in the precipitate, d^0 the number of constitutive defects, and δ the atomic volume misfit between the precipitate and the matrix.

In Fig. 6 we represent a cluster space similar to that of paper I Fig. 1, where the locus of those clusters with zero associated strain energy is represented. (A very large atomic volume misfit has been assumed.) What we suggest is that the incoherency of the precipitate matrix interface simply introduces a particular s dependence of the defect-solute cluster binding energy. Such a dependence was ignored in paper I.

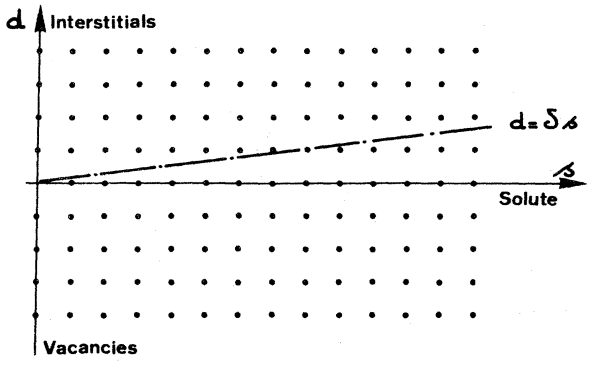

FIG. 6. Cluster space for incoherent clusters; —·— clusters with zero associated strain energy.

C. Further comments on cluster trajectories

Despite its success, the model depicted in paper I is very crude indeed. If it yields the right criterion for solid solution metastability it does not give any details on the actual trajectories of the clusters in the (d,s) plane. In other words we know why a critical cluster size exists, but we ignore the mechanism by which a cluster reaches the critical size. Since in an undersaturated solid solution, large solute clusters are rare, and since the incubation time for radiation-induced precipitation is rather short (cf. Table I) it might be that interstitial clusters form very frequently and are destroyed by frequent arrival of vacancy solute complexes: the vacancy-interstitial recombination would leave in place solute clusters close enough to the critical size to have a good chance of getting supercritical. [One of us (G.M.) is indebted to Dr. M. Baron for enlightening discussion on this point.]

D. Homogeneous versus heterogeneous radiation-induced precipitation

As a summary, homogeneous radiation-induced precipitation is accounted for by the irreversibility of the vacancy-interstitial mutual recombination reaction at solute clusters. On the other hand heterogeneous radiation-induced precipitation, (heterogeneous means here "at point-defect sinks") was successfully accounted for by the elimination of point defects at point-defect sinks.[3,6,25] Do the above two modes of precipitation compete in a given system? In the NiSi system only *heterogeneous* γ' precipitation was reported,[37] except at low temperature and high flux where the precipitation was so dense that it was not possible to recognize dislocation loops by strain contrast of the transmission electron micrographs.[6] but the occurrence of γ' precipitate-dislocation loop association could not be ruled out. Similarly, in the NiGe system, γ' radiation-induced precipitation is reported to be always heterogeneous.[7] In the AlZn system just discussed, Zn precipitation was observed to be only homogeneous. It must be recognized, however, that dislocation loops are rare and that very few grain boundaries have been observed. We cannot completely rule out the occurrence of heterogeneous precipitation in this system but if there is any, it is not the dominant feature.

Can we specify under what conditions homogeneous rather than heterogeneous induced precipitation is expected to prevail? In a qualitative way, one may suggest that homogeneous radiation-induced precipitation is triggered in a regime where the elimination of point defects occurs mainly by mutual recombination, while heterogeneous radiation-induced precipitation develops when the elimination of point defects occurs mainly at fixed sinks. Indeed, as shown by

the Johnson-Lam model[25] no solute segregation to point-defect sinks occurs under irradiation conditions such that vacancy-interstitial mutual recombination is very prominent. On the other hand, the homogeneous precipitation model presented in paper I operates when recombination is prominent (mainly at solute clusters).

We are aware of the crude level of the above argument. In particular we do not explain the reason why no homogeneous radiation-induced γ' precipitation is observed in NiSi at low temperature where heterogeneous precipitation does not occur. Radiation-induced disordering and dissolution have not been included in the model and might be necessary, as discussed elsewhere.[6]

V. SUMMARY AND CONCLUSIONS

AlZn dilute solid solutions containing from 0.2 to 4.4 at.% Zn have been irradiated with high-flux 1-MeV electrons at temperatures well within the solid solubility of Zn in Al. GP zones or Zn precipitates are observed to form under appropriate irradiation conditions (flux and temperature), yielding the definition of a flux-dependent solvus of Zn in Al. When radiation-induced precipitation occurs, the precipitate volume fraction saturates before the matrix composition has reached the solubility limit under irradiation just defined. The existing models of radiation-induced precipitation fail to account for the above observations.

The model of vacancy-interstitial recombination induced solid-solution metastability presented in paper I does account for the results, both qualitatively and with the right order of magnitude, although with a slight overestimation of the effect of irradiation. For assessing the latter model, a new computation scheme of the point-defect population in a solid solution under irradiation has been developed, where the single-phase solid solution is treated as an average medium.

The reasons why the model overestimates the effect of irradiation have been discussed in a qualitative way. Improvements are suggested. More accurate values of solute-interstitial complex migration energies are needed. Despite these weaknesses, the success of the model suggests that the dominant mechanism for radiation-induced homogeneous precipitation is the *irreversible* recombination of mixed interstitials with vacancy-solute complexes, and that the coherency or noncoherency at the precipitate matrix interface plays only a minor role in this problem.

Radiation-induced homogeneous precipitation is therefore thought to be an example of so-called nonequilibrium phase transition.

ACKNOWLEDGMENTS

We gratefully acknowledge the stimulating interest of Dr. Y. Adda in this work, the cooperation of Dr. A. Barbu and J. L. Bocquet who gave access to unpublished work, and useful discussions with or technical assistance of Dr. M. Baron, Dr. N. Q. Lam, Dr. M. Marot, and Dr. K. Urban.

APPENDIX A

1. Diffusion in a dilute binary alloy in the presence of vacancies only

As is well known[18,38] the currents of A and B atoms under isothermal conditions are written

$$J_A = L_{AA}(X_A - X_V) + L_{AB}(X_B - X_V) \ , \qquad J_B = L_{BA}(X_A - X_V) + L_{BB}(X_B - X_V) \ , \tag{A1}$$

and the vacancy current is

$$J_V = -(J_A + J_B) \ . \tag{A2}$$

L_{ij} are phenomenological coefficients and X_i the thermodynamical driving forces, the expression of which is given in Refs. 18 and 38. However for the sake of clarity, we rewrite these expressions using variables of interest in the irradiation problem, namely, the concentration of *free* vacancies and of *free* solute atoms which we call, respectively, c_V and c_B. If we call a the lattice parameter, using the standard indices for the five basic vacancy jump frequencies in a fcc dilute solution and noting that the concentration of solute-vacancy complexes c_p is given by

$$c_p = k_V c_V c_B \tag{A3}$$

with

$$k_V = 12\frac{W_4}{W_3} \ , \tag{A4}$$

we obtain

$$L_{AA} = N\frac{a^2}{kT} W_0 c_V \left[1 + c_B\left(7 - \frac{W_4}{W_0}\frac{40(W_1+W_3)+4W_2(W_1/W_3+7/2)}{W_1+W_2+7/2\,W_3}\right)\right] \ , \tag{A5a}$$

$$L_{AB} = L_{BA} = N\frac{a^2}{kT} c_V c_B \frac{2W_2W_4(3/2 - W_1/W_3)}{W_1+W_2+7/2\,W_3} \ , \tag{A5b}$$

$$L_{BB} = \frac{a^2}{kT} N c_V c_B \frac{W_2W_4(W_1/W_3+7/2)}{W_1+W_2+7/2\,W_3} \ , \tag{A5c}$$

where N is the number of lattice sites per unit volume. The thermodynamic driving forces are given by

$$X_i = -\nabla \mu_i \ . \tag{A6}$$

The expressions of μ_V, μ_B, μ_A as a function of the concentrations of *free* vacancies and *free* solute are

$$\mu_V = \mu_V^0 + kT \ln c_V + kT(Zc_B + c_p) \ , \tag{A7a}$$

$$\mu_B = \mu_B^0 + kT \ln c_B + kT(Zc_V + c_p) \ , \tag{A7b}$$

$$\mu_A = \mu_A^0 - kT(c_V + c_B + c_p) \ . \tag{A7c}$$

According to Eq. (A3), we know that

$$\nabla c_p / c_p = \nabla c_V / c_V + \nabla c_B / c_B \ . \tag{A8}$$

With the aid of Eqs. (A6) to (A8) we may rewrite Eq. (A1) as

$$\frac{J_B}{kT} = (L_{AB} + L_{BB}) \frac{\nabla c_V}{c_V} + [(1+Z)c_B L_{AB} - (1 - Zc_B) L_{BB}] \frac{\nabla c_B}{c_B} \ , \tag{A9a}$$

$$\frac{J_V}{kT} = -(L_{AA} + L_{BB}) \frac{\nabla c_V}{c_V} - [(1+Z)c_B L_{AA} + L_{AB} - (1 - Zc_B) L_{BB}] \frac{\nabla c_B}{c_B} \ , \tag{A9b}$$

where we have neglected c_V and c_p when compared to c_B, and c_B when compared to 1 but not Zc_B compared to 1 (Z is the number of nearest neighbors: 12 in fcc crystals).

The solute and vacancy fluxes J_B and J_V can also be expressed in terms of the gradients of the total vacancy and solute concentrations, respectively, $\mathcal{C}_V$ and $\mathcal{C}_B$ defined by

$$\mathcal{C}_V = c_V + c_p \ , \tag{A10a}$$

$$\mathcal{C}_B = c_B + c_p \ , \tag{A10b}$$

$$\frac{J_B}{kT} = \frac{L_{AB} + L_{BB}}{\mathcal{C}_V} \nabla \mathcal{C}_V + \left[\left((1+Z) - \frac{k_V}{1 + k_V \mathcal{C}_B} \right) L_{AB} + \left(Z - \frac{1}{\mathcal{C}_B} - \frac{k_V}{1 + k_V \mathcal{C}_B} \right) L_{BB} \right] \nabla \mathcal{C}_B \ , \tag{A11}$$

$$\frac{J_V}{kT} = -\frac{L_{AA} + 2L_{AB} + L_{BB}}{\mathcal{C}_V} \nabla \mathcal{C}_V - \left[\left((1+Z) - \frac{k_V}{1 + k_V \mathcal{C}_B} \right) L_{AA} + \left(Z - \frac{1}{\mathcal{C}_B} - \frac{k_V}{1 + k_V \mathcal{C}_B} \right) L_{BB} + \left((1+2Z) - \frac{1}{\mathcal{C}_B} - \frac{k_V}{1 + k_V \mathcal{C}_B} \right) L_{AB} \right] \nabla \mathcal{C}_B \ . \tag{A12}$$

Following Ref. 18 we define a vacancy diffusion coefficient in the dilute solid solution, $\mathfrak{D}_V$ such that

$$J_V = -\mathfrak{D}_V \nabla N \mathcal{C}_V \tag{A13}$$

in the absence of solute concentration gradient ($\nabla \mathcal{C}_B = 0$). From Eq. (A12), we have

$$\mathfrak{D}_V = \frac{kT}{N} \frac{L_{AA} + 2L_{AB} + L_{BB}}{\mathcal{C}_V} \ , \tag{A14}$$

or according to Eq. (A5)

$$\mathfrak{D}_V(\mathcal{C}_B) = \frac{D_V}{1 + k_V \mathcal{C}_B} \left[1 + \mathcal{C}_B \left(7 - \frac{W_4}{W_0} \frac{40(W_1 + W_3) + W_2(7W_1/W_3 + 9/2)}{W_1 + W_2 + 7W_{3/2}} \right) \right] \ , \tag{A15}$$

where $D_V = a^2 W_0$ is the vacancy diffusion coefficient in the pure solvent, and since $\mathcal{C}_B \sim c_B$, we have used

$$\mathcal{C}_V = c_V (1 + k_V \mathcal{C}_B) \ . \tag{A16}$$

Similarly, the diffusion coefficient of the solute B by the vacancy mechanism $\mathfrak{D}_S^V$ is deduced from Eq. (A9a), setting $\nabla c_V = 0$

$$J_B = -\mathfrak{D}_S^V \nabla \mathcal{C}_B \ . \tag{A17}$$

Again assuming $\mathfrak{C}_B \sim c_B$, we get

$$\mathfrak{D}_S^V(\mathfrak{C}_B) = kT\left[(1-Z\mathfrak{C}_B)\frac{L_{BB}}{\mathfrak{C}_B} - (1+Z)L_{AB}\right] . \tag{A18}$$

With the aid of expressions (A5), we get

$$\mathfrak{D}_S^V(\mathfrak{C}_B) = \frac{c_V}{c_V^0} D_B{}^*(0) \times \left[1-\mathfrak{C}_B\left[Z+2(1+Z)\frac{3/2 - W_1/W_3}{W_1/W_3 - 7/2}\right]\right] , \tag{A19}$$

where $D_B{}^*(0)$ is the solute diffusion coefficient in the pure metal, and c_V^0 the vacancy thermal equilibrium concentration. The discrepancy between Eq. (A19) and the original formula[18] results from the fact that the terms in $Z\mathfrak{C}_B$ were not neglected compared to 1. In Eq. (A19), we have

$$D_B{}^*(0) = a^2 c_V^0 \frac{W_4 W_2 (W_1 + 7/2\, W_3)}{W_3 W_1 + W_2 + 7/2\, W_3} . \tag{A20}$$

The useful result for Sec. III is that

$$\mathfrak{D}_S^V(\mathfrak{C}_B) = D_B{}^*(\mathfrak{C}_B)\frac{c_V}{c_V^0} . \tag{A21}$$

2. Numerical values for the effective vacancy diffusion coefficient

In order to evaluate the effective vacancy diffusion coefficient $\mathfrak{D}_V(\mathfrak{C}_B)$ in the AlZn solid solution [Eq. (A15)] we can rely on four experimental determinations: (i) the vacancy diffusion coefficient in pure Al (D_V) as deduced from self-diffusion data and vacancy concentration data in pure Al (Ref. 14); (ii) the sign of the solute drift by vacancy flow[39]; (iii) the dependence of the Al self-diffusion coefficient on Zn content[40]; (iv) the Zn diffusion data in pure Al.[19] In the next section, we show that $\mathfrak{D}_V(\mathfrak{C}_B) < D_V/(1+k_V\mathfrak{C}_B)$.

a. Solute drift by vacancy flow is known to be positive in AlZn (Ref. 31)

According to Eq. (A11), in the absence of solute concentration gradient ($\nabla\mathfrak{C}_B = 0$), the solute flux is

$$J_B = kT(L_{AB} + L_{BB})\nabla\mathfrak{C}_V/\mathfrak{C}_V \tag{A22}$$

$$= -kT\frac{W_1 - \frac{13}{2}W_3}{W_1 + \frac{7}{2}W_3}\frac{\nabla\mathfrak{C}_V}{\mathfrak{C}_V} . \tag{A23}$$

We therefore deduce that

$$\frac{W_1}{W_3} > \frac{13}{2} . \tag{A24}$$

b. Variation of the Al diffusion coefficient with the Zn content

The tracer diffusion coefficient of the solvent in a dilute solid solution is[41]

$$D_A{}^*(\mathfrak{C}_B) = D_A{}^*(0)(1+b\mathfrak{C}_B) . \tag{A25}$$

If we neglect the $\mathfrak{C}_B$ dependance of the correlation factor for self-diffusion, b is given by

$$b = -18 + \frac{W_4}{W_3}\frac{4W_1 + 14W_3}{W_0} . \tag{A26}$$

From published data[40] one may deduce[42]

$$b \simeq -3.75 . \tag{A27}$$

Equation (A24) together with Eq. (A27) yields

$$\frac{W_4}{W_0} < 0.36 . \tag{A28}$$

c. Zn tracer diffusion data in pure Al

The best available data[19] show that W_2 and W_0 have nearly the same activation energy. Introducing Eqs. (A24) and (A27) into Eq. (A15) shows that in the two limiting cases $W_2 \ll W_1$ and W_3, or $W_2 \gg W_1$ and W_3, the following relation holds

$$\mathfrak{D}_V(\mathfrak{C}_B) < \frac{D_V}{1+k_V\mathfrak{C}_B} . \tag{A29}$$

In the following, we take $\mathfrak{D}_V(\mathfrak{C}_B)$ equal to the right-hand side of Eq. (A29).

3. Extension to solute diffusion by dumbbell mechanism

As established recently,[21] the same type of development as in Eq. (A1) can be performed for diffusion by the dumbbell mechanism. The resulting expressions are

$$\mathfrak{D}_i(\mathfrak{C}_B) = \frac{D_i(0)(1+\beta_i\mathfrak{C}_B) + k_{pa}\gamma_{pa}\mathfrak{C}_B}{1+k_i\mathfrak{C}_B} , \tag{A30}$$

where $D_i(0)$ is the diffusion coefficient of interstitials in the pure solvent, k_i is an overall trapping coefficient of interstitials at solute atoms, β_i, K_{pa}, and γ_{pa} only depend on the various jump frequencies of the dumbbell in the vicinity of the solute atom, the ex-

pression of which is not important here. Similarly

$$D_S^i(\mathfrak{C}_B) = c_i[K_{pa}D_{pa}(1+k_i\mathfrak{C}_B)+2\sigma_i D_i(0)k_i\mathfrak{C}_B] \ , \tag{A31}$$

where D_{pa} and σ_i are also given as functions of the dumbbell jump frequencies.[21] k_i is given by

$$k_i = k_{pa}+k_{pB}+k_{BI} \ , \tag{A32}$$

where k_{pa}, k_{pB}, and k_{BI} are the equilibrium constants of the following reactions:

$$\text{self-interstitial}+\text{solute} \overset{k_{pa}}{\longleftrightarrow} \text{type } a \text{ complex} \ ,$$

$$\text{type } a \text{ complex} \overset{k_{BI}}{\longleftrightarrow} \text{mixed dumbbell} \ ,$$

$$\text{self-interstitial}+\text{solute} \overset{k_{pB}}{\longleftrightarrow} \text{type } b \text{ complex} \ .$$

Type a and b complexes are solute interstitials nearest-neighbor configurations which, respectively, may or may not transform into mixed dumbbell within one jump of the interstitial.

APPENDIX B: POINT-DEFECT CONCENTRATIONS IN SOLID SOLUTIONS UNDER IRRADIATION

1. Single-phase solid solution

We assume that in the single-phase solid solution, the solute atoms are all isolated. Equations (A15) and (A30) allow for the definition of effective vacancy and interstitial diffusion coefficient in the solid solution. By analogy with the point-defect balance equations in pure metals, under irradiation, we write

$$\frac{\partial \mathfrak{C}_v}{\partial t} = G - \mathfrak{R}_{iv}\mathfrak{C}_i\mathfrak{C}_v - K_v(\mathfrak{C}_v-\mathfrak{C}_v^0) \ , \tag{B1}$$

$$\frac{\partial \mathfrak{C}_i}{\partial t} = G - \mathfrak{R}_{iv}\mathfrak{C}_i\mathfrak{C}_v - K_i\mathfrak{C}_i \ , \tag{B2}$$

where $\mathfrak{C}_i$ and $\mathfrak{C}_v$ are the vacancy and interstitial (free and associated with single solute atoms) concentrations, G the production rate of defects, R_{iv} an effective rate constant for interstitial-vacancy mutual recombination

$$\mathfrak{R}_{iv} = 4\pi r_0(\mathfrak{D}_i+\mathfrak{D}_v)/\Omega \tag{B3}$$

(where r_0 is the recombination radius and Ω the Al atomic volume), and K_v (respectively, K_i) is the rate constant for vacancy (respectively, interstitial) elimination at dislocations

$$K_v = \mathfrak{D}_v Z_v \rho_d \ , \tag{B4a}$$

$$K_i = \mathfrak{D}_i Z_i \rho_d \tag{B4b}$$

(where ρ_d is the dislocation density and Z_v and Z_i efficiency factors).

Note that for the thin foils used in the high voltage electron microscope irradiations, the dominant sinks are the foil surfaces, which are equivalent to a dislocation density of $\rho_d = \pi^2/e^2$ where e is the foil thickness[43] with $Z_i = Z_v = 1$. Finally $\mathfrak{C}_v^0$ in Eq. (B1) is the thermal equilibrium vacancy concentration. From Eqs. (B1) and (B2), we get at steady state

$$\mathfrak{C}_i = \frac{K_v}{K_i}(\mathfrak{C}_v-\mathfrak{C}_v^0) \ , \tag{B5}$$

which together with Eq. (B1) gives

$$\mathfrak{C}_v = \tfrac{1}{2}\mathfrak{C}_v^0\left[(1-\zeta)+(1+\zeta)\left(1+\frac{4G}{K_v\mathfrak{C}_v^0}\frac{\zeta}{(1+\zeta)^2}\right)^{1/2}\right] \ , \tag{B6}$$

where

$$\zeta = \frac{K_i}{R_{iv}\mathfrak{C}_i^0} \ . \tag{B7}$$

As usual two regimes may be distinguished: (i) the recombination regime where $\zeta << 1$ and

$$\mathfrak{C}_v \simeq \tfrac{1}{2}\mathfrak{C}_v^0\left[1+\left(1+\frac{4Z_iG}{Z_vR_{iv}\mathfrak{C}_v^{0^2}}\right)^{1/2}\right] \tag{B8}$$

and (ii) the sink elimination regime where $\zeta >> 1$ and

$$\mathfrak{C}_v \simeq \tfrac{1}{2}\mathfrak{C}_v^0\zeta\left[-1+\left(1+\frac{4G}{K_v\mathfrak{C}_v^{0^2}}\frac{1}{\zeta}\right)^{1/2}\right] \ . \tag{B9}$$

2. Two-phase solid solution

In the model under consideration the only effect of precipitates on the point-defect concentrations is to introduce fixed traps (the sites at the precipitate-matrix interface) in the defect balance equations. These traps are saturable and independent in the sense that the binding energy of a point-defect at a trap does not depend on the occupation probability of neighbor traps. The trapping centers can therefore be treated as homogeneously distributed in the matrix. The appropriate balance equations for vacancies, interstitials in the matrix ($\mathfrak{C}_v$,$\mathfrak{C}_i$), and at traps ($\mathfrak{C}_{vt}$,$\mathfrak{C}_{it}$) are given in the text [Eqs. (6a)–(6d)]. According to Sec. 1 of Appendix B, we give the new rate constants of Eqs. (6a)–(6d) the following expressions:

$$\mathfrak{R}_{vt} = 4\pi r_{vt}\mathfrak{D}_v/\Omega \ , \tag{B10}$$

$$\mathfrak{R}_{it} = 4\pi r_{it}\mathfrak{D}_i/\Omega \ , \tag{B11}$$

$$K_v'' = 4\pi r_{vt}'\mathfrak{D}_v/\Omega \ , \tag{B12}$$

$$K_i'' = 4\pi r_{it}'\mathfrak{D}_i/\Omega \ , \tag{B13}$$

$$K_v' = (\mathfrak{D}_v/a^2)\exp(+g_v^b/kT) \ , \tag{B14}$$

$$K_i' = (\mathfrak{D}_i/a^2)\exp(+g_i^b/kT) \ . \tag{B15}$$

In the above equations r_{vt} (respectively, r_{it}) is the recombination radius for a trapped vacancy (respectively, interstitial) with a mobile interstitial (respectively, vacancy); r'_{vt} (respectively, r'_{it}) is the capture radius of a trap for vacancies (respectively, interstitials); and g_v^b (respectively, g_i^b) is the binding energy of a vacancy (respectively, interstitial) at a trap. $g^b < 0$ for an attractive interaction.

For the sake of simplicity we assume

$$r_{vt} = r_{it} = r'_{vt} = r'_{it} = \tfrac{1}{2} r_0 \quad . \tag{B16}$$

The factor $\frac{1}{2}$ stems from the fact that trapping centers at a precipitate matrix interface can be reached from approximately one half space only.

At steady state Eqs. (6a) to (6d) can be rearranged by simple algebra to give Eq. (8) with the following expressions of the coefficients:

$$a_1 = \mathcal{C}_v^0 \left[\frac{(\alpha+1)(\hat{k}_i' + \hat{k}_v') - (3\alpha^2+2\alpha+1)}{\alpha^2+\alpha+1} + \frac{\hat{k}_v}{\alpha \mathcal{R}'} + \frac{(\alpha+1)}{(\alpha^2+\alpha+1)} \frac{\mathcal{C}_t}{\mathcal{R}'} \right] , \tag{B17}$$

$$a_2 = \mathcal{C}_v^{0^2} \left[\frac{\hat{k}_i' \hat{k}_v' - (2\alpha+1)(\hat{k}_i' + \hat{k}_v') + \alpha(3\alpha+1)}{\alpha^2+\alpha+1} + \frac{\hat{k}_v[(\alpha+1)(\hat{k}_i' + \hat{k}_v') - (3\alpha^2+2\alpha+1)]}{\alpha(\alpha^2+\alpha+1)\mathcal{R}'} \right.$$
$$\left. + \frac{\hat{k}_i' + \hat{k}_v' - (2\alpha+1)}{(\alpha^2+\alpha+1)\mathcal{R}'} \mathcal{C}_t - \frac{G'}{\alpha \mathcal{R}'} \right] , \tag{B18}$$

$$a_3 = \mathcal{C}_v^{0^3} \left[\hat{k}_v \frac{[\hat{k}_i' \hat{k}_v' - (2\alpha+1)(\hat{k}_i' + \hat{k}_v') + \alpha(3\alpha+1)]}{\alpha(\alpha^2+\alpha+1)\mathcal{R}'} - \frac{\hat{k}_i' \hat{k}_v' - \alpha(\hat{k}_i' + \hat{k}_v') + \alpha^2}{\alpha^2+\alpha+1} \right.$$
$$\left. - \frac{(\hat{k}_i' + \hat{k}_v' - \alpha)\mathcal{C}_t}{(\alpha^2+\alpha+1)\mathcal{R}'} - \frac{[(\alpha+1)(\hat{k}_i' + \hat{k}_v') - \alpha(2\alpha+1)]P'}{\alpha(\alpha^2+\alpha+1)\mathcal{R}'} \right] , \tag{B19}$$

$$a_4 = \mathcal{C}_v^{0^4} \left[- \frac{(G' + \hat{k}_v)[\hat{k}_i' \hat{k}_v' - \alpha(\hat{k}_i' + \hat{k}_v') + \alpha^2]}{\alpha(\alpha^2+\alpha+1)\mathcal{R}'} \right] . \tag{B20}$$

The following notation is used

$$\mathcal{R}_v = 2\pi r_0 \mathcal{D}_v / \Omega = \mathcal{R}_{it} = K_v'' \quad , \tag{B21}$$

$$\mathcal{R}_i = 2\pi r_0 \mathcal{D}_i / \Omega = \mathcal{R}_{vt} = K_i'' \quad , \tag{B22}$$

$$\hat{k}_v = K_v / \mathcal{R}_v, \quad \hat{k}_i = K_i / \mathcal{R}_i, \quad \alpha = \hat{k}_v / \hat{k}_i \quad , \tag{B23}$$

$$\mathcal{R} = \mathcal{R}_{iv} / \mathcal{R}_i \mathcal{R}_v \quad , \tag{B24}$$

$$\mathcal{C}_v^{0'} = \mathcal{R}_v \mathcal{C}_v^0 \quad , \tag{B25}$$

$$G' = G / \mathcal{C}_v^{0'}, \quad \mathcal{R}' = \mathcal{R} / \mathcal{C}_v^{0'}, \quad \hat{k}_i' = K_i' / \mathcal{C}_v^{0'}, \quad \hat{k}_v' = K_v' / \mathcal{C}_v^{0'} \quad , \tag{B26}$$

$\mathcal{C}_t$ is the density of trapping centers. The solution of Eq. (8) is known in analytical form.

---

[1]R. Cauvin and G. Martin, Phys. Rev. B 23, 3322 (1981) (preceding paper).
[2]R. Cauvin and G. Martin, J. Nucl. Mater. 83, 67 (1979).
[3]P. R. Okamoto, A. Taylor, and H. Wiedersich, in Fundamental Aspects of Radiation Damage in Metals, edited by M. T. Robinson and F. W. Young, in Proceedings of the U.S. ERDA Conference No. 75, 1975 (unpublished), p. 1188.
[4]A. Barbu and A. J. Ardell, Scr. Metall. 9, 1233 (1975).
[5]A. Barbu and G. Martin, Scr. Metall. 11, 771 (1977).
[6]A. Barbu, CEA Report No. R-4936.
[7]A. Barbu, in Proceedings of the International Conference

on irradiation behavior of metallic materials for fast reactor core components, 1979, edited by J. Poirier and J. M. Dupouy (unpublished), p. 69.
[8]S. I. Maydet and K. C. Russell, J. Nucl. Mater. 64, 101 (1977).
[9]H. Hansen, *Constitution of Binary Alloys* (McGraw-Hill, London, 1958).
[10]J. L. Bocquet and G. Martin, J. Nucl. Mater. 83, 186 (1979).
[11]J. H. Gittus and A. P. Miodownik, J. Nucl. Mater. 85 and 86, 621 (1979).
[12]C. H. P. Lupis and H. Gaye, Metall. Trans. 6, 1049 (1975).
[13]L. Kaufman (private communication).
[14]J. Hillairet, *Defauts ponctuels dans les solides* (Editions de Physique, Orsay, France, 1977), p. 417.
[15]W. Schilling, J. Nucl. Mater. 69 and 70, 465 (1978).
[16]M. S. Saidefar and K. C. Russell, J. Nucl. Mater. 85 and 86, 931 (1979).
[17]K. C. Russell, Nucl. Mater. 83, 176 (1979).
[18]R. E. Howard and A. B. Lidiard, Rep. Prog. Phys. 27, 161 (1964).
[19]N. L. Peterson and S. J. Rothman, Phys. Rev. B 1, 3264 (1970).
[20]I. Godeny, D. Beke, F. J. Kedyes, and G. Groma, Phys. Status Solidi (a) 32, 195 (1975).
[21]A. Barbu, Acta Metall. 28, 199 (1980).
[22]P. H. Dederichs, C. Lehmann, H. R. Schober, A. Scholz, and R. Zeller, J. Nucl. Mater. 69 and 70, 176 (1978).
[23]L. E. Rehn, K. H. Robrock, and H. Jacques, J. Phys. F 8, 1835 (1978).
[24]N. Q. Lam, N. V. Doan, and Y. Adda, J. Phys. F 10, 2359 (1980).
[25]R. A. Johnson and N. Q. Lam, Phys. Rev. B 13, 4364 (1976).
[26]L. K. Mansur, J. Nucl. Mater. 83, 109 (1979).
[27]J. Takamura, M. Koike, and K. Furukawa, J. Nucl. Mater. 69 and 70, 738 (1978).
[28]F. W. Young, Jr., J. Nucl. Mater. 69 and 70, 310 (1978).
[29]H. W. King, J. Mater. Sci. 1, 79 (1966).
[30]C. J. Smithells, *Metals Reference Handbook* (Plenum, New York, 1967).
[31]M. R. Mruzik and K. C. Russell, J. Nucl. Mater. 78, 343 (1978).
[32]H. M. Simpson and R. L. Chaplin, Phys. Rev. 185, 958 (1969).
[33]A. Bartels, F. Dworschak, H. P. Meurer, C. Abomeit, and H. Wollenberger, J. Nucl. Mater. 83, 24 (1979).
[34]H. Wollenberger, J. Nucl. Mater. 69 and 70, 362 (1978).
[35]K. C. Russell, Scr. Metall. 3, 313 (1969).
[36]M. V. Speight, Metal. Sci. J. 6, 107 (1972).
[37]K. Jonghorban and A. J. Ardell, J. Nucl. Mater. 85 and 86, 719 (1979), have reported homogeneous coherent γ' RIP in NiSi alloys. This precipitation, however, is confined in a region of inhomogeneous defect production rate and might result from a solute redistribution on a scale much coarser than the size of the precipitates themselves [N. Q. Lam (private communication)].
[38]R. E. Howard and A. B. Lidiard, Philos. Mag. 11, 1179 (1965).
[39]T. R. Anthony, in *Diffusion in Solids,* edited by A. S. Nowick and J. J. Burton (Academic, New York, 1975), p. 353.
[40]T. G. Stoebe, R. D. Gulliver, II, T. O. Ogurtani, and R. A. Huggins, Acta Metall. 13, 701 (1965).
[41]A. B. Lidiard, Philos. Mag. 5, 1049 (1960).
[42]J. L. Bocquet (unpublished).
[43]G. J. Dienes and G. H. Vineyard, *Radiation Effects in Solids* (Interscience, New York, 1957), p. 138.